Available online at www.sciencedirect.com
SCIENCE DIRECT®
Journal of Crystal Growth 262 (2004) 151–156
JOURNAL OF CRYSTAL GROWTH
www.elsevier.com/locate/jcrysgro

MOCVD growth of AlN/GaN DBR structures under various ambient conditions

H.H. Yao, C.F. Lin, H.C. Kuo, S.C. Wang*

Institute of Electro-optical Engineering, National Chiao Tung University, Hsinchu 300, Taiwan

Received 17 July 2003; accepted 17 October 2003
Communicated by C.R. Abernathy

Abstract

The high-reflectivity AlN/GaN distributed Bragg reflector (DBR) structures were realized by metal organic chemical vapor deposition (MOCVD) growth under pure N_2 ambient for AlN epilayer growth. The highest peak reflectivity of about 94.5% with a stopband width of 18 nm at a center wavelength of 442 nm was obtained. For the DBR structure with AlN layer grown under mixture of N_2/H_2 and pure H_2 conditions, the center wavelength was blue-shifted to 418 and 371 nm and the peak reflectivity also showed a reduction to 92% and 79%, respectively. The stopband width also decreases with increasing H_2 contents. The surface roughness and the grain size of the grown DBR structures showed an increase with increasing the H_2 ambient gas ratio. For realization of a high reflectivity and broad bandwidth of AlN/GaN DBR by using the MOCVD growth method, the pure N_2 ambient gas for growth of AlN layer should be preferable and optimal condition.

PACS: 78.55.Cr; 42.55.Sa; 42.55.Px

Keywords: Distributed Bragg reflector; AlN; GaN; MOCVD; Ambient gas

1. Introduction

Gallium nitride is a direct wide band-gap semiconductor which has attracted great attention because of applications in fabrication of light sources of short wavelengths. In particular, GaN-based semiconductor laser diodes (LDs) and light-emitting diodes (LEDs) have applications in displays, traffic signals, and high-density digital versatile disks (HD-DVD). The blue GaN-based LEDs and edge emitting LDs have been developed in recent years. The research interest has gradually shifted to the development and demonstration of GaN-based vertical cavity surface emitting lasers (VCSELs) [1–4] and resonant-cavity light-emitting diodes (RCLEDs) [5–10]. An important requirement for the operation of such devices is the need of high reflectance mirrors, usually in the form of distributed Bragg reflectors (DBRs). The VCSELs require highly reflective DBR mirrors on both sides of the active region to form the laser cavity, while for the RCLEDs the high reflectance DBRs can improve the output power and emission spectrum.

*Corresponding author.
E-mail address: scwang@cc.nctu.edu.tw (S.C. Wang).

0022-0248/$ - see front matter © 2003 Elsevier B.V. All rights reserved.
doi:10.1016/j.jcrysgro.2003.10.062

The DBR structures are particular important for GaN VCSELs in two aspects. First, according to Honda et al. [11], the threshold current density of a GaN VCSEL can be reduced by an order of magnitude with an increase of the DBR peak reflectance from 90% to 99%. Therefore, the DBRs with high reflectivity are necessary for VCSELs. The second aspect is that the DBRs should have large stopband width. This is important because the active region of the GaN-based VCSEL is typical made of InGaN multiple quantum wells (MQWs), and the emission peak of the InGaN MQWs tends to fluctuate with small variations in either the growth conditions or the process parameters [12–14]. The DBRs with wide stopband can provide sufficient coverage of such spectral variation in emission wavelength.

The main difficulty in fabrication of GaN-based DBRs with high reflectivity and large stopband width is the small index of refraction contrast that can be obtained within the entire AlGaN alloy compositions. As a result, a large number of pairs are required to achieve the high reflectivity. In addition, the large lattice mismatch between GaN and AlGaN tends to create a lot of tensile stress induced cracks during the growth of the DBR structure resulting in reduced reflectivity and increase in scattering loss. Several GaN/AlGaN-based DBR structures have been reported previously. These DBRs were either grown by molecular beam epitaxy (MBE) [15–17] or by metal organic chemical vapor deposition (MOCVD) [18–20]. Among these, Figiel and coworkers [19] reported the control and elimination of the tensile growth stress by insertion of multiple AlN interlayers in the GaN/AlGaN DBR structures and demonstrated the crack-free growth of 60 pairs of $Al_{0.20}Ga_{0.80}N$/GaN DBR mirrors over the entire 2 in wafer with a maximum reflectivity of at least 99%, but the stopband width was only 13 nm.

In order to reduce the number of pairs and increase the mirror stopband, high index of refraction contrast material pairs using AlN/GaN were also reported using the MBE [21–23] and MOCVD system [24]. However, the lattice mismatch between AlN and GaN ($\sim$2.4%) and the large different of thermal expansion coefficients between GaN (5.59×10^{-6}/K) and AlN (4.2×10^{-6}/K) could lead to the crack formation. Using the plasma-assisted MBE, Ng et al. [22] reported the network of cracks on AlN/GaN DBR can be reduced or complete eliminated by the asymmetric DBR structures and obtained a peak reflectance of up to 99% centered at 467 nm with a wide bandwidth of 45 nm. However, it is relatively difficult for the MOCVD system to grow good structural quality and high-reflectivity AlN/GaN DBR structures, because of the difficulty in the control of the epitaxial layer thickness due to much complex chemical processes and changes on the surface conditions. For example, the onset temperature for GaN decomposition is lower in H_2 ambient compared to other ambient conditions such as N_2, Ar and vacuum [25]. Yamaguchi et al. [26] reported that using N_2 as a carrier gas, AlN can release the strain energy between the GaN interface by the generation of misfit dislocation, not by that of a network of cracks. Hence, using the MOCVD system to grow AlN/GaN DBR structures is relatively difficult and the peak reflectance obtained so far was only about 88% [24].

In this paper, we report the study of the ambient gas effect during the growth of AlN in AlN/GaN DBR structures by the MOCVD system. The optimal growth conditions of AlN/GaN DBRs for obtaining high optical and structural quality with high reflectivity and wide stopband width were established.

2. Experiments

The GaN/AlN DBRs are grown on the polished optical-grade C-face (0 0 0 1) 2″ diameter sapphire substrates by the MOCVD system (EMCORE D-75). Trimthylgallium (TMGa) and trimthylaluminum (TMAl) were used as Ga and Al sources, respectively, and ammonia (NH_3) was used as N source. A thermal cleaning process was carried out at 1080°C for 10 min in a stream of hydrogen ambient before the growth of epitaxial layers. After depositing of a 30-nm-thick GaN nucleation layer at 530°C, the temperature was raised up to 1045°C for the growth of a 1-μm-thick GaN buffer

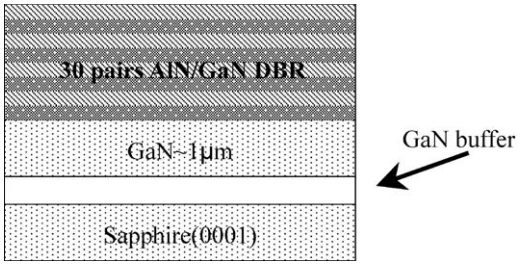

Fig. 1. Schematic structures of a 30-pair AlN/GaN DBR.

layer. The flow rate of TMGa was 89.5 μmol/min and the flow rate of NH_3 was 3.6 l/min. Then a 30-pair AlN/GaN DBR structure was grown at 1040°C under the fixed chamber pressure of 100 Torr. During the growth of GaN and AlN epitaxial layers for the DBR structures, the growth times of GaN and AlN layer were fixed at 85 and 528 s, respectively, and the flow rates of TMAl, TMGa, NH_3 were set at 74.9 μmol/min, 71.6 μmol/min and 1.2 l/min, respectively. By fixing the GaN growth condition in H_2 ambient gas with a H_2 flow rate of 3400 sccm, the AlN layer was grown under three differential ambient gas conditions. Sample A was grown in N_2 ambient gas, sample B was grown in N_2 and H_2 mixture ambient gas (with a 35% H_2 gas), and sample C was grown in H_2 ambient gas. The ambient gas flow rate was fixed at 3400 sccm. The schematic structure of the grown DBR is shown in Fig. 1. The surface morphology and epitaxial thickness of AlN layers were measured by atomic force microscopy (AFM), optical microscopy (OM) and transmission electron microscopy (TEM). The reflectivity spectrum of the AlN/GaN DBR structure was measured by the n&k ultraviolet–visible spectrometer with normal incidence at room temperature.

3. Results and discussion

The surface images of the grown AlN/GaN DBR samples observed by the OM with 200 × magnification are shown in Fig. 2. All these samples showed a crack-free surface over the whole 2 in wafer. We also measured the surface morphology of three samples by AFM and the measurement results are shown in Table 1. The

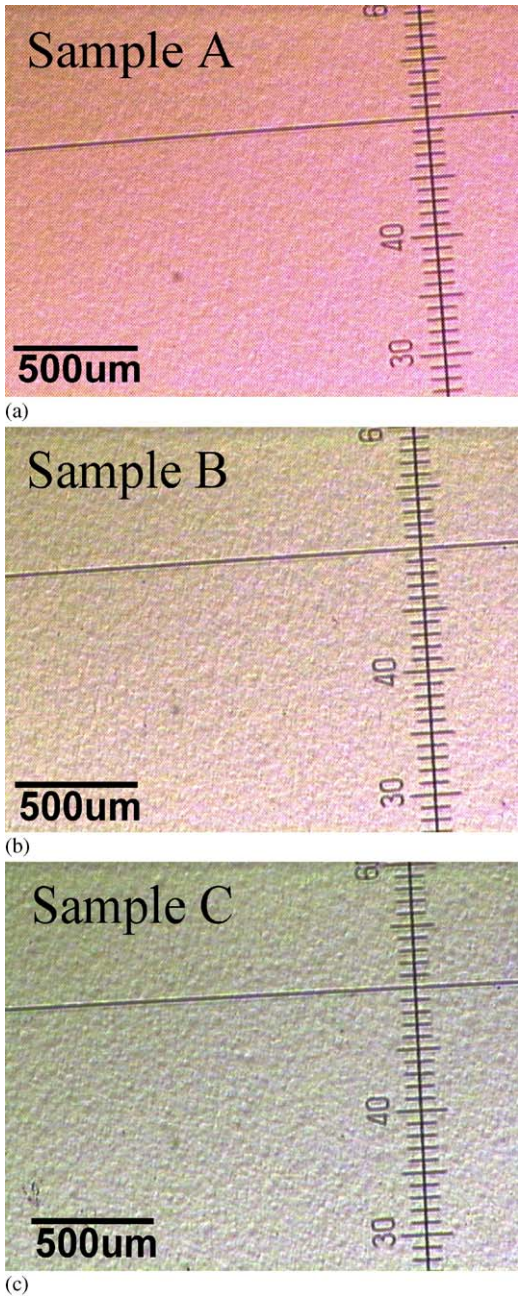

Fig. 2. Optical microscope images with 200 × magnification of (a) sample A, (b) sample B and (c) sample C.

surface roughness of these DBR samples increased from 8.1, 10.7, to 12.4 with increasing the H_2 gas content, and the grain size also increased from 2, 8, to 10 μm for samples A, B, and C, respectively.

Table 1
Surface morphology of samples A, B and C observed by atomic force microscopy

Sample	Surface roughness R_a (nm)	Grain size (μm)	H_2 component (5)
A	8	2	0
B	10	5	35
C	12	10	100

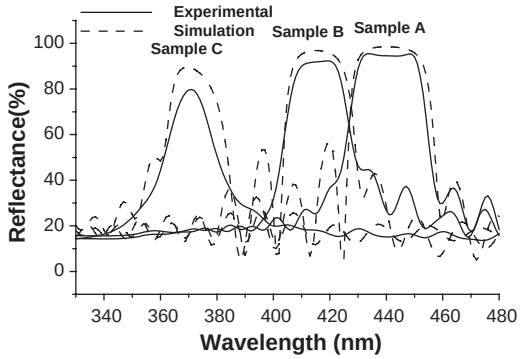

Fig. 3. Experimental optical reflectance spectra of three 30-pair AlN/GaN DBR (solid lines) and numerical simulations of the optical reflectance spectra (dash lines).

The reflectivity spectra of samples A, B, and C were shown in Fig. 3 (solid line). Sample A showed the highest reflectivity of about 94.5% with peak wavelength at 442 nm and a stopband width of 18 nm. Sample B showed a decrease in the peak reflectivity to about 92% at a blue-shifted peak wavelength of 418 nm with a stopband width of 13 nm. For sample C, the peak reflectivity was further decreased to 79.7% with a narrower stopband width of only 6 nm at a peak wavelength further blue-shifted to 371 nm.

To investigate the blue-shifted in the peak wavelength of the DBRs, the cross-section TEM images of these three samples were investigated. Fig. 4(a) shows the TEM image of the entire DBR structure (30 periods) of Sample A. The lighter and the darker layers are the GaN layers and AlN layers, respectively. The dislocation defect was observed in the bottom GaN bulk layer, but the dislocations did not extend into the DBR structure. Moreover, the TEM image also showed no observable cracks. The thicknesses of the AlN and

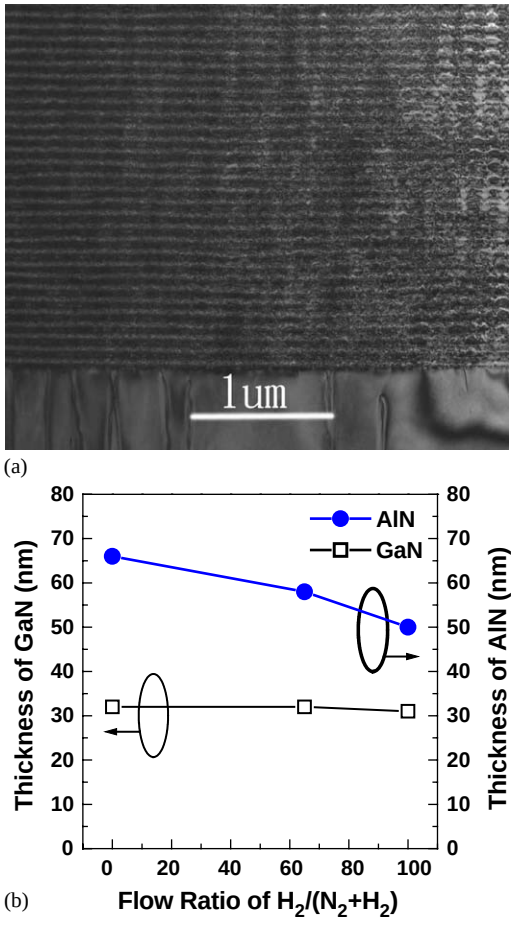

Fig. 4. TEM analysis results. (a) Cross-section TEM image of sample A. The darker layers are AlN while the lighter layers are GaN. (b) Thickness of AlN and GaN layers in these three DBR samples.

GaN epitaxial layer estimated from the TEM pictures of three samples are shown in Fig. 4(b). The thickness of AlN layers shows a gradual decrease from 66, 60, to 50 nm for samples A, B, and C, respectively. The result suggests that the blue-shifted in the peak wavelength of the DBRs could be caused by the thickness decreasing of the AlN layers. Furthermore, the thickness of the grown AlN layer for the three samples was almost two times that of the GaN layer indicating the asymmetric nature of the DBRs. The observed crack-free surface of these samples could be the result of the relaxation of the tensile stress in the

asymmetric structures as reported by Ng et al. [22]. Based on the thickness data we estimate the growth rate of AlN layer and obtained a gradual decrease of growth rate from 1.25 Å/s for sample A in pure N_2 ambient gas, 1.10 Å/s for sample B in N_2/H_2 mixture ambient gas and to 0.95 Å/s for sample C in pure H_2 ambient gas. The lower AlN growth rate in H_2 ambient gas than that in N_2 ambient gas could be due to the higher AlN decomposition rate in H_2 ambient gas than that in N_2 ambient gas. This phenomenon was also observed by Koleske et al. [25] during the growth of GaN layer.

Using the thickness data obtained from the TEM analysis, we simulated the reflectivity spectra of the DBR structures using the transfer matrix method and fitted with the experimental spectra. The refraction index values for GaN and AlN material were adapted from the published data [27]. Since the center DBR wavelengths of these samples are all near the GaN bandedge, the estimated GaN absorption coefficient values of 150, 200 and 3385 cm^{-1} for wavelength at 440, 418 and 371 nm, respectively, from the published data of Yu et al. [28] are also used. The simulation results are plotted along with the experimental data in Fig. 3 (dash line). Table 2 lists the peak reflectivity and the peak wavelength based on the simulation results and comparison with the experimental data. The simulation results suggest that the AlN layer thickness variation is a major contributing factor in the blue-shift of the peak wavelength. Besides the variation in the AlN layer thickness, the different in the surface roughness of the DBRs as observed by the AFM could also contribute to the reduction in peak reflectivity and the bandwidth narrowing of the DBR structures.

From these experiment results, the H_2 ambient gas content during the growth of AlN layers in AlN/GaN DBR structures has a strong influence on the optical and structural quality of the DBR structures grown by MOCVD. For obtaining high reflectivity and wide stopband width of AlN/GaN DBR structures by MOCVD, the best condition is to grow AlN layers in the N_2 ambient gas environment.

4. Conclusions

In conclusion, the high-reflectivity AlN/GaN DBR structures were obtained by MOCVD growth under pure N_2 ambient gas for growth of AlN epilayers. The highest peak reflectivity of about 94.5% with a stopband width of 18 nm at center wavelength of 442 nm was obtained. For the DBR structure with AlN layer grown under mixture N_2/H_2 and H_2 conditions, both the peak reflectivity and the stopband width were decreased and the center wavelengths of the DBR structures were blue-shifted. Therefore for realization of a high reflectivity and broad bandwidth of AlN/GaN DBR by using the MOCVD growth method, the pure N_2 ambient gas for growth of AlN layer should be the preferable and optimal condition.

Acknowledgements

This research was supported by the National Science Council of Taiwan, ROC, under Contract No. NSC 90-2215-E-009-102 and by the Ministry of Education of Taiwan, ROC under Contract No. 88-FA06-AB. The authors would like to thank Y.C. Hsien of Department of Materials Science

Table 2
Comparison of the experimental and simulated peak reflectance values of these three 30-pair AlN/GaN distributed Bragg reflectors

Sample	Experimental (%)		Simulation (%)	
	Peak reflectance (%)	Center wavelength (nm)	Peak reflectance (%)	Center wavelength (nm)
A	94.5	442	98.5	440
B	92.0	418	96.9	415
C	79.9	371	89.5	369

and Engineering, National Chiao Tung University for the TEM experiment supporting.

References

[1] T. Honda, A. Katsube, T. Sakaguchi, F. Koyama, K. Iga, Jpn. J. Appl. Phys. Pt. 1 24 (1995) L3527.
[2] J.M. Redwing, D.A.S. Loeber, N.G. Anderson, M.A. Tischler, J.S. Flynn, Appl. Phys. Lett. 69 (1996) 1.
[3] T. Someya, K. Tachibana, J.K. Lee, T. Kamiya, Y. Arakawa, Jpn. J. Appl. Phys. Pt. 2 37 (1998) L1424.
[4] I.L. Krestnikov, W.V. Lundin, A.V. Sakharov, V.A. Semenov, A.S. Usikov, A.F. Tsatsul'nikov, Zh.I. Alferov, N.N. Ledentsov, A. Hoffmann, D. Bimberg, Appl. Phys. Lett. 75 (1999) 1192.
[5] Y.-K. Song, H. Zhou, M. Diagne, I. Ozden, A. Vertikov, A.V. Nurmikko, C. Carter-Coman, R.S. Kern, F.A. Kish, M.R. Krames, Appl. Phys. Lett. 74 (1999) 3441.
[6] Y.-K. Song, M. Diagne, H. Zhou, A.V. Nurmikko, C. Carter-Coman, R.S. Kern, F.A. Kish, M.R. Krames, Appl. Phys. Lett. 74 (1999) 3720.
[7] Y.-K. Song, M. Diagne, H. Zhou, A.V. Nurmikko, R.P. Schneider Jr., T. Takeuchi, Appl. Phys. Lett. 77 (2000) 1744.
[8] N. Nakada, M. Nakaji, H. Ishikawa, T. Egawa, M. Umeno, T. Jimbo, Appl. Phys. Lett. 76 (2000) 1804.
[9] S. Fernández, F.B. Naranjo, F. Calle, M.A. Sánchez-Garćýa, E. Calleja, P. Vennegues, A. Trampert, K.H. Ploog, Semicond. Sci. Technol. 16 (2001) 913.
[10] F.B. Naranjo, S. Fernańdez, M.A. Sańchez-Garcýá, F. Calle, E. Calleja, Appl. Phys. Lett. 80 (2002) 2198.
[11] T. Honda, A. Katsube, T. Sakaguchi, F. Koyama, K. Iga, Jpn. J. Appl. Phys. Pt. 1 34 (1995) 3527.
[12] H.M. Ng, T.D. Moustakas, S.N.G. Chu, Appl. Phys. Lett. 76 (2000) 281.
[13] R. Singh, D. Doppalapudi, T.D. Moustakas, L.T. Romano, Appl. Phys. Lett. 70 (1997) 1089.
[14] D. Doppalapudi, S.N. Basu, T.D. Moustakas, J. Appl. Phys. 85 (1999) 883.
[15] R. Langer, A. Barski, J. Simon, N.T. Pelekanos, O. Konovalov, R. Andre, Le Si Dang, Appl. Phys. Lett. 74 (1999) 3610.
[16] S. Fernandez, F.B. Naranjo, F. Calle, M.A. Sanchez-Garcia, E. Calleja, P. Vennegues, A. Trampert, K.H. Ploog, Appl. Phys. Lett. 79 (2001) 2136.
[17] F. Natali, D. Byrne, A. Dussaigne, N. Grandjean, J. Massies, B. Damilano, Appl. Phys. Lett. 82 (2003) 499.
[18] T. Someya, Y. Arakawa, Appl. Phys. Lett. 73 (1998) 3653.
[19] K.E. Waldrip, J. Han, J.J. Figiel, H. Zhou, E. Makarona, A.V. Nurmikko, Appl. Phys. Lett. 78 (2001) 3205.
[20] H.P.D. Schenk, P. de Mierry, P. Vennegues, O. Tottereau, M. Laugt, M. Vaille, E. Feltin, B. Beaumont, P. Gibart, S. Fernandez, F. Calle, Appl. Phys. Lett. 80 (2002) 174.
[21] I.J. Fritz, T.J. Drummond, Electron. Lett. 31 (1995) 68.
[22] H.M. Ng, T.D. Moustakas, S.N.G. Chu, Appl. Phys. Lett. 76 (2000) 2818.
[23] F. Natali, N. Antoine-Vincent, F. Semond, D. Byrne, L. Hirsch, A. Serge Barrière, M. Leroux, J. Massies, J. Leymarie, Jpn. J. Appl. Phys. Pt. 2 41 (2002) L1140.
[24] T. Shirasawa, N. Mochida, A. Inoue, T. Honda, T. Sakaguchi, F. Koyama, K. Iga, J. Crystal Growth 189–190 (1998) 124.
[25] D.D. Koleske, A.E. Wickenden, R.L. Henry, J.C. Culbertson, M.E. Twigg, J. Crystal Growth 223 (2001) 466.
[26] S. Yamaguchi, M. Kosaki, Y. Watanabe, Y. Yukawa, S. Nitta, H. Amano, I. Akasaki, Appl. Phys. Lett. 79 (2001) 3062.
[27] D. Brunner, H. Angerer, E. Bustarret, F. Freudenberg, R. Hopler, R. Dimitrov, O. Ambacher, M. Stutzmann, J. Appl. Phys. 82 (1997) 5090.
[28] G. Yu, G. Wang, H. Ishikawa, M. Umeno, T. Soga, T. Egawa, J. Watanabe, T. Jimbo, Appl. Phys. Lett. 70 (1997) 3209.